

# Chalmers interferometric test using a reflective spatial light modulator

B. Canales-Pacheco,\* A. Cornejo-Rodríguez, and F. Granados-Agustín

Instituto Nacional de Astrofísica Óptica y Electrónica, Apartado Postal 51 y 216, Puebla PUE 72000, México.

\*canales321@inaoep.mx

**Abstract:** In this paper, we propose the use of a reflective spatial light modulator (RSLM) controlled by a PC, instead of a metal plate with holes, to produce the interference patterns in Chalmers interferometric test. The main advantage of the proposed method is that with an RSLM, it is possible to test and obtain an interference pattern for any zone of a surface or lens by opening two appropriate apertures. This increases the accuracy of the results and reduces the time required to obtain them.

©2012 Optical Society of America

**OCIS codes:** (220.4840) Optical design and fabrication; (120.3180) Instrumentation, measurement, and metrology.

---

## References and links

1. L. C. Martin, "The testing of optical instruments, and the study of their performance," in *Technical Optics* (Pitman, 1959), 285–286.
2. M. Antonieta Zuloaga Garmendia, *Chalmers Test*. Masters in Science thesis, Instituto Nacional de Astrofísica, Óptica y Electrónica, México (1994).
3. F. Granados Agustín, J. Fausto Escobar Romero, and A. Cornejo Rodríguez, "Testing parabolic surface with annular subaperture interferograms," *Opt. Rev.* **11**(2), 82–86 (2004).
4. F. Granados Agustín and A. Cornejo Rodríguez, "Generalización del método de mediciones interferométricas múltiples en pruebas de superficies ópticas," *Rev. Mex. Fis.* **45**(2), 132–139 (1999).
5. J. Liesener and H. J. Tiziani, "Interferometer with dynamic reference," in *Optical Fabrication, Testing, and Metrology*, R. Geyl, D. Rimmer, L. Wang, eds., Proc. SPIE **5252**, 264 (2004).
6. J. Kacperski and M. Kujawinska, "Active, LCoS based laser interferometer for microelements studies," *Opt. Express* **14**(21), 9664–9678 (2006).
7. C. Gardner and A. H. Bennett, "A modified Hartmann test based on interference," *J. Opt. Soc. Am.* **11**(4), 441–452 (1925).
8. F. A. Jenkins and H. E. White, "Interference of two beams of light," in *Fundamentals of Optics* (McGraw Hill, 1981), 261–266.
9. M. Born and E. Wolf, "Elements of the theory of interference and interferometers," in *Principles of Optics* (Cambridge, 1999), 286–292.
10. H. Guenther and D. H. Liebenberg, "Automatic techniques for analyzing nulled interferograms," in *Optical Interferograms Reduction and Interpretation*, R. C. Moore eds (ASTM, Philadelphia, 1978), 34–35.
11. M. V. Mantravadi and D. Malacara, "Newton, Fizeau and Haidinger interferometers," in *Optical Shop Testing*, D. Malacara ed. (A. John Wiley & Sons, 2007), 12–13.

---

## 1. Introduction

The Chalmers test, described by Martin [1], is shown in Fig. 1, where a set of holes are made in a rigid screen located at the exit pupil of a lens under test. The procedure proposed by Chalmers is to use two adjacent holes each time the test is carried out, and observe the produced interferogram by these holes. The lens can be tested along a vertical line by using a pair of holes at a time and shifting a horizontal slit.

In a more recent work, Zuloaga [2] performed the Chalmers test by using a lithographic technique to make holes in the Chalmers screen. One disadvantage of the classical Chalmers test is the tedious work that has to be done in order to obtain quantitative results. Moreover, this test involves the use of the stitching technique [3, 4] and was probably the first practical application of this technique. The stitching technique is required to integrate the partial information of the interferograms produced by each pair of holes.

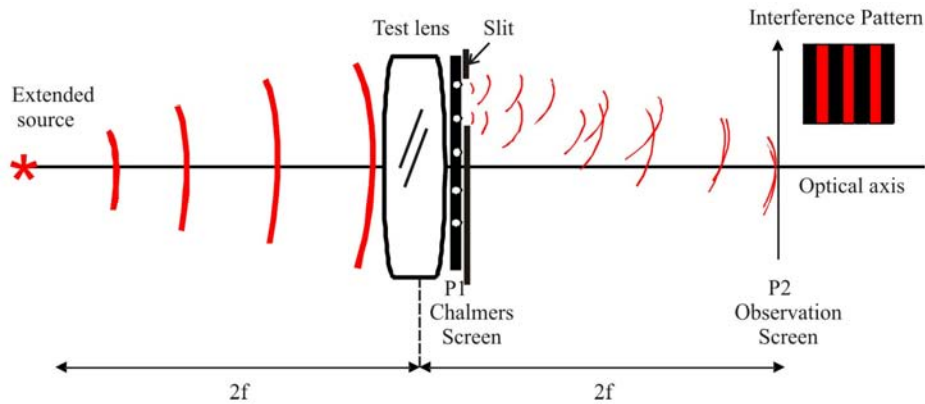


Fig. 1. Diagram of the Chalmers test.

A study similar to the present one was performed by Liesener and Tiziani [5], who used a spatial light modulator (SLM) to extend the dynamic range of interferometric measurements for testing surfaces with strong asphericities. They proposed using a Twyman–Green interferometer and placing an SLM in the path of the reference beam to introduce a tilt in the  $x$  or  $y$  directions. This allows the modification of the phase and results in an interferogram with a low spatial frequency. Another similar work was presented by Kacperski and Kujawinska [6]. They modified the classical Twyman Green interferometer and placed an SLM in the path of the reference beam; this device was designed to act as a mirror that allows the introduction of an arbitrary phase. In particular, they analyzed interferograms produced by  $0.45 \times 0.45 \text{ mm}^2$  and  $1.35 \times 1.35 \text{ mm}^2$  micromembranes. As already mentioned, the main proposal in this paper is to use the principle of the Chalmers test for analyzing only the local defects on an optical surface. A previous study in this direction was conducted by Gardner and Bennett [7] using a Hartmann screen. They obtained local information from interference patterns produced by shifting the Hartman screen along the optical axis.

In the technique proposed here, a reflective spatial light modulator (RSLM) is used, which allows the screen to remain at a fixed position, and only two apertures are used at a time. It is convenient to mention that in the present work and the works by Chalmers and Gardner and Bennett, the working principle is Young's interference experiment [8], that can be applied for testing any spheric or aspheric surfaces. It is worth mentioning that the main difference between our method and the well established interferometric tests is that whereas the other methods obtain a global evaluation of the wavefront arriving from the optical element or surface being tested, the here proposed method allows that local or zonal defects in the wavefront are analyzed. On the other hand, instead of producing the Chalmers screen on a rigid metal sheet, the use of an RSLM provides a very flexible way of selecting a particular zone to be tested. The advantage of the proposed kind of dynamic Chalmers test is that using an RSLM, it is possible to select a pair of holes to be made in real time, for any zone, and also with different sizes and orientation of the holes, as shown Fig. 2.

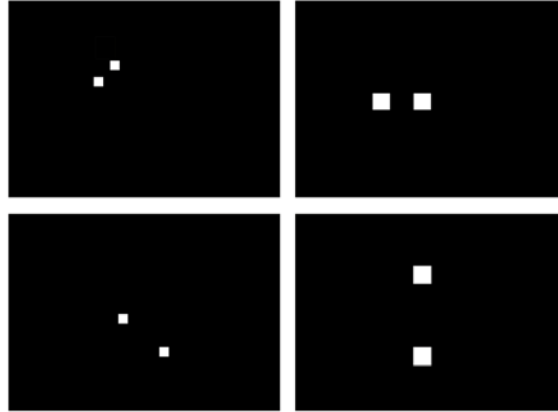


Fig. 2. Selection of open holes with different positions, separations, and size.

## 2. Theory for Chalmers test

From the widely accepted theory of interference, which postulates that interference occurs due to wavefront division [9], it is known that if two monochromatic waves  $E_1$  and  $E_2$  are superimposed at some point  $P$  (Fig. 3) the total intensity at  $P$  is

$$I = I_1 + I_2 \pm 2\sqrt{I_1 I_2} \cos \delta, \quad (1)$$

where  $\delta$  is the phase difference and  $I_1$   $I_2$  are the intensities such that

$$I_1 = \langle E_1^2 \rangle \quad I_2 = \langle E_2^2 \rangle. \quad (2)$$

As is well known, the relation between the phase difference  $\delta$  and the optical path difference  $\Delta$  is

$$\delta = \frac{2\pi}{\lambda} \Delta = \frac{2\pi}{\lambda} (\overline{BP} - \overline{AP}), \quad (3)$$

where  $\overline{BP}$  and  $\overline{AP}$  are the optical paths distances from the holes  $A$  and  $B$  to point  $P$  on the screen, according to the Young experiment [8] and Fig. 3. If we evaluate the relative phases at  $P$  in terms of the distance  $h$  from the central point  $P_0$ , the separation  $a$  between the apertures  $A$  and  $B$ , and the distance  $d$  from the apertures to the observing screen, then

$$\Delta = a \sin \alpha = a \frac{h}{d}. \quad (4)$$

Substituting Eq. (4) into Eq. (3), a relation between the experimental parameters,  $a$ ,  $d$ , and  $h$  is obtained, as follows:

$$h = \lambda \frac{d}{a}. \quad (5)$$

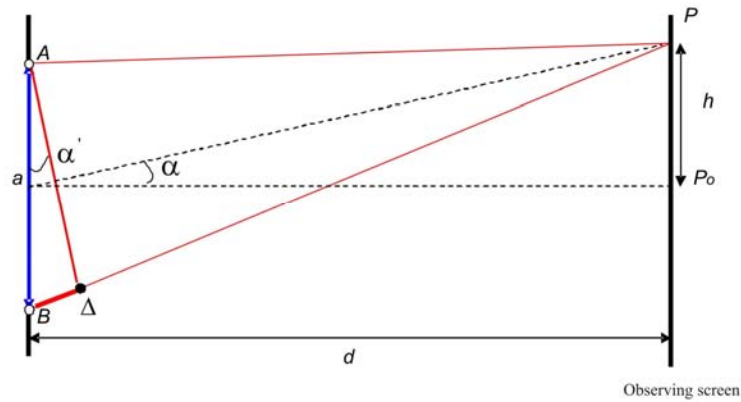


Fig. 3. Geometry of wavefront propagation in the Young's experiment.

### 3. Experimental setup and best conditions to produce interferograms

The RSLM used is the model SXGA-R2, from Forth Dimension Display, with the following specifications: 1280 x 1024 pixels, with a pixel size of 13.62  $\mu\text{m}$  and a total area of 17.43 x 13.95 mm. Figure 2 shows how two "holes" or apertures can be opened using the RSLM at any position and with different orientations. This makes it feasible to test specific small zones on the surface under test, as will be shown in what follows.

Figure 4 shows the experimental arrangement for testing a concave spherical surface by means of the reflective characteristic of the RSLM device. The light source used is a He-Ne laser with a power of 2 mW. The spherical surface under test has a radius of curvature of 60 cm and a diameter of 13 cm. The RSLM is located in front of the center of curvature at a distance of 53 cm and is inclined at a certain angle with respect to the optical axis of the surface. Such positioning of the RSLM allows the interference pattern to be observed and recorded using a CCD camera so that it can be stored in a computer. The CCD camera model used is XCST50 (768 (H) x 494 (V) pixels), from Hitachi, Ltd.

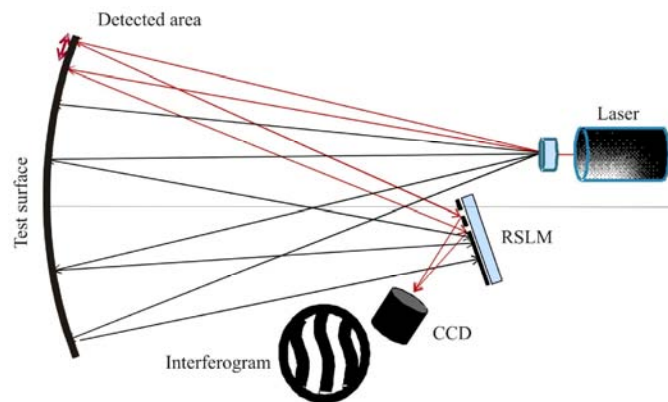


Fig. 4. Experimental diagram of the proposed method.

Figures 5(a), 5(b) and 5(c) show the kind of interferograms that can be produced depending upon the alignment, size, and the separation of the holes on the RSLM. Our study was performed using the experimental scheme in Fig. 4.

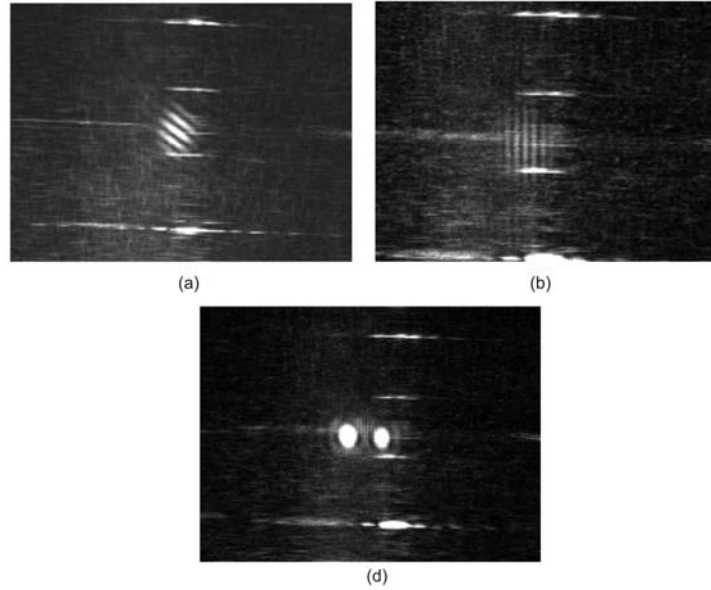


Fig. 5. (a) Interference pattern produced by two squares of size  $554\ \mu\text{m}$ , aligned at  $45^\circ$  and separated by  $1088\ \mu\text{m}$ ; (b) interference pattern produced by two circles of size  $408\ \mu\text{m}$ , separated by  $1360\ \mu\text{m}$ , and with vertical alignment; (c) interference pattern produced by two circles of size  $1360\ \mu\text{m}$ , separated by  $2720\ \mu\text{m}$ , and with vertical alignment.

We investigated the best size and separation of the apertures for observing interferograms with good visibility. Table 1 lists the number of fringes observed for various aperture sizes and distances. We also investigated ways of improving the contrast of the fringes. Figures 6 and 7 show examples of apertures with the same separation of 50 pixels, but with different sizes, 20 and 40 pixels respectively. For 20 pixel apertures, Fig. 6, the interference pattern is best observed for the 8th diffraction order. For 40 pixel apertures, Fig. 7, the pattern is best observed for the 7th diffraction order, Fig. 7.

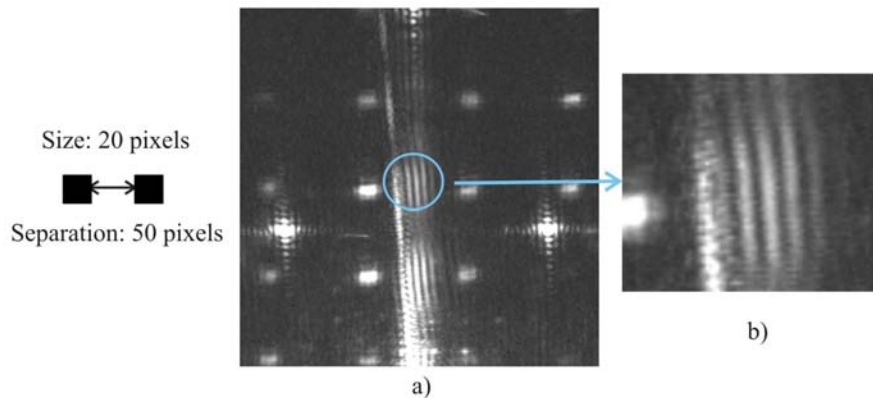


Fig. 6. (a) Interference with squares of size 20 pixels ( $272\ \mu\text{m}$ ), separated by 50 pixels ( $680\ \mu\text{m}$ ). (b) Amplification of the interferogram of the eighth order of diffraction.

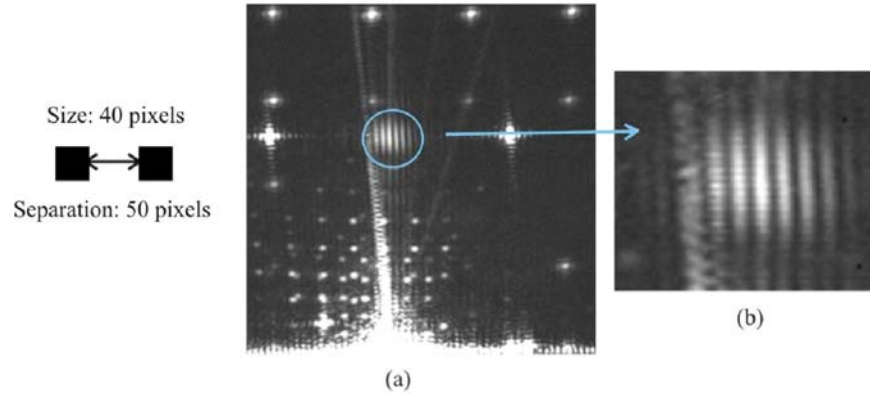


Fig. 7. (a) Interference with squares of size 40 pixels (544  $\mu\text{m}$ ), separated by 50 pixels (680  $\mu\text{m}$ ). (b) Amplification of the interferogram of the seventh order of diffraction.

**Table 1. Results obtained with different sizes and separations of aperture squares in the RSLM.**

Size of squares ( $\mu\text{m}$ )	Separation of ( $\mu\text{m}$ )	Number of fringes
136	136	1
136	272	4
136	408	6
136	544	8
136	680	9
272	136	3
272	272	3
272	408	4
272	544	5
272	680	6
272	816	7
272	952	8
408	136	3
408	272	3
408	408	3
408	544	4
408	680	5
408	816	7
408	952	8
544	136	3
544	272	3
544	408	3
544	544	4
544	680	5
544	816	7
544	952	8
680	136	1
680	272	3
680	408	3
680	544	3
680	680	4
680	816	6
680	952	8

#### 4. Experimental results for the testing of an optical surface

Before giving the experimental results, we are going to explain how zonal errors are localized on the surface under test. Figure 8 shows the present experimental setup on a pneumatic table. Figure 9 describes how a set of two crossed slits are fixed close to the surface. The slits are mounted on slide mechanical devices.

Figure 10 shows an observed interferogram produced by a Fizeau commercial interferometer (ZYGO™), by displaying a set of localized deformations on the surface. In regards to the particular zones on the mirror, as shown in Fig. 10, some numbers were assigned according to the square mesh shown in Fig. 11. The mesh is fixed on the flat back surface of the tested transparent reflective surface. Therefore, with the combination of the two slits in Fig. 9 and the square mesh in Fig. 11, it was possible to identify the particular zones to be tested.

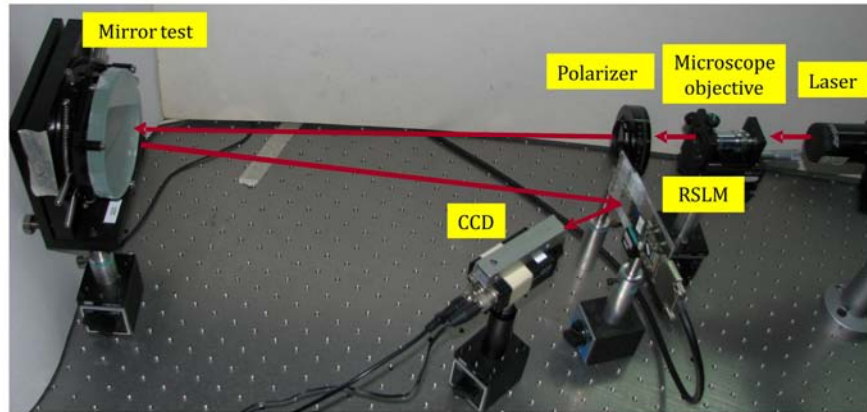


Fig. 8. Experimental setup.

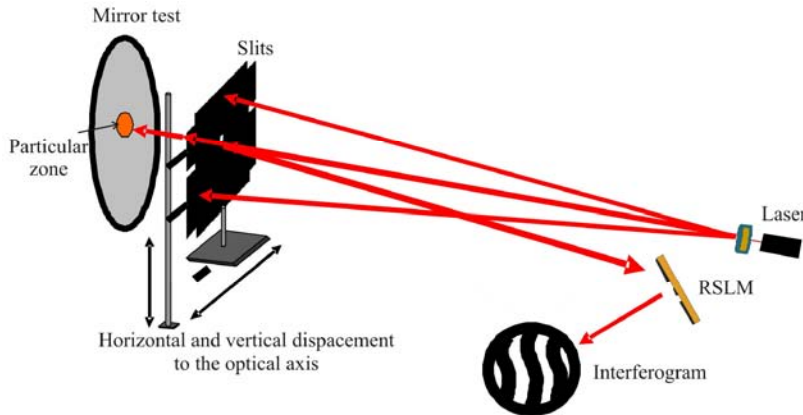


Fig. 9. Selection of the wavefront.

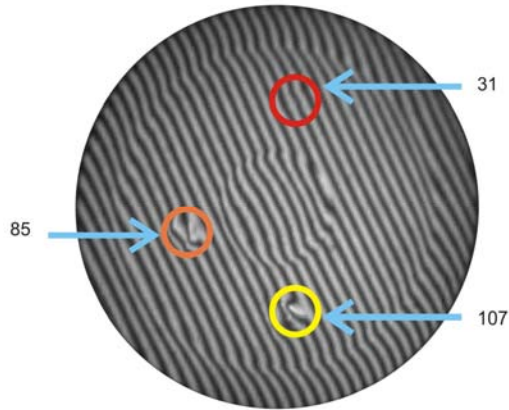


Fig. 10. Interferogram test of mirror with 5 deformations.

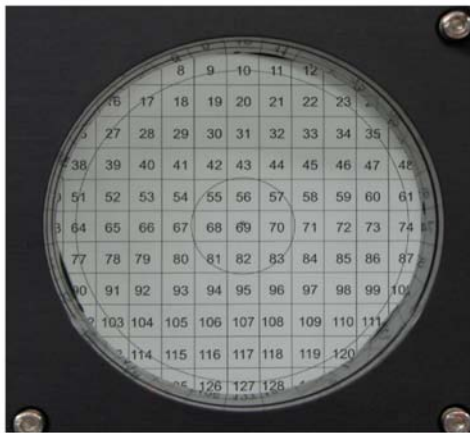


Fig. 11. Mesh location of interferograms.

In order to obtain our experimental results from the zonal interferograms shown in Figs. 12 (a), 12(b) and 12(c), as a first approach, we performed a quantitative analysis of the results derived from the proposed method. The deviations of the interference fringes from a straight line were calculated, according to the equation of Guenther [10]:

$$surface\ error = Es = \frac{\Delta S \left( \frac{\lambda}{2} \right)}{S}, \quad (6)$$

where  $\Delta S$  is the separation between two experimental interference fringes and the straight line and  $S$  is the distance between the dark fringes. The error in our measurements with the applied method becomes less than  $\lambda/2$ . Taking into account that our measurements are the so called peak error described by Mantravadi and Malacara [11].

An important aspect of our proposal for testing zone errors, it is the fact that a numbers of fringes that can be observed in the defect areas. For the case of the Fizeau interferometer, Fig. 10, only one fringe is observed for each zone. For the interferograms of Fig. 12, several fringes can be observed. Additionally, the resolution is better for the analysis of the interferograms from the method of Fig. 12.

In Table 2 are listed the final results for the zones 31, 107 and 85 as described in Fig. 10. For each one of the interferograms of Figs. 12(a), 12(b) and 12(c), the patterns with better contrast were chosen.

**Table 2. Derived error for the three tested zones of the spherical mirror.**

Zone No.	Surface error	Fig.
31	$0.07\lambda$	12.a
107	$0.51\lambda$	12.b
85	$0.44\lambda$	12.c

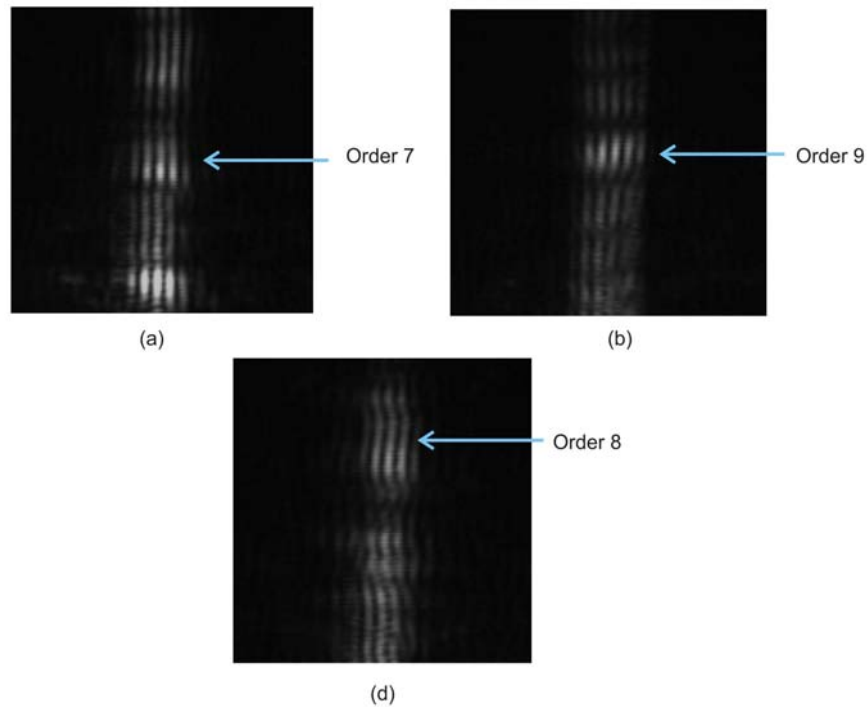


Fig. 12. (a) Interference with vertical oriented squares of size 40 pixels ( $544\ \mu\text{m}$ ) and separated by 40 pixels ( $544\ \mu\text{m}$ ) in zone 31; (b) interference with squares of size 40 pixels ( $544\ \mu\text{m}$ ) and separated by 40 pixels ( $544\ \mu\text{m}$ ) in zone 107; (c) interference with squares of size 40 pixels ( $544\ \mu\text{m}$ ) and separated by 40 pixels ( $544\ \mu\text{m}$ ) in zone 85.

## 5. Conclusions

It is worth mentioning, that in order to obtain satisfactory interferograms for performing the measurements, appropriate values of aperture size and separation must be determined. For the results in Table 2, the size of the apertures was  $544\ \mu\text{m}$  and the distance between them was  $544\ \mu\text{m}$ .

To our knowledge, the experimental proposal presented in this paper, to evaluate small zonal errors on an optical surface, is an innovative and alternative technique based on the method proposed by Chalmers many years ago. In order to obtain the experimental results derived here, it was necessary to: a) understand how a RSLM works, b) determine the effect of the size of the apertures and their separation based on the Young's experiment, and c) observe different diffraction orders produced by RSLM in order to obtain interference fringes

with high contrast. Of course, it is possible that another method may be used for identifying the zones, instead of the method using crossed slits and the square mesh described here.

### **Acknowledgments**

B. Canales acknowledges the financial support from CONACyT, Mexico, under scholarship no. 205190. The authors are grateful to the reviewers for very import comments to our original text.